Supporting information

Large Pulsed Electron Beam Welded Percolation Networks of Silver Nanowires for Transparent and Flexible electrodes

Jisoo Kim,[†] *Yun Seok Nam,*[‡] *Myoung Hoon Song,*[*,‡] *Hyung Wook Park*[*,†]

[†]School of Mechanical and Nuclear Engineering, [‡]School of Materials Science and Engineering and KIST-UNIST Ulsan Center for Convergent Materials, Ulsan National Institute of Science and Technology (UNIST), UNIST-gil 50, Eonyang-eup, Ulju-gun, Ulsan, Republic of Korea, 44919.

Corresponding Author

*E-mail (M.H.S.): mhsong@unist.ac.kr

*E-mail (H.W.P.): hwpark@unist.ac.kr

Contents

Section S1.

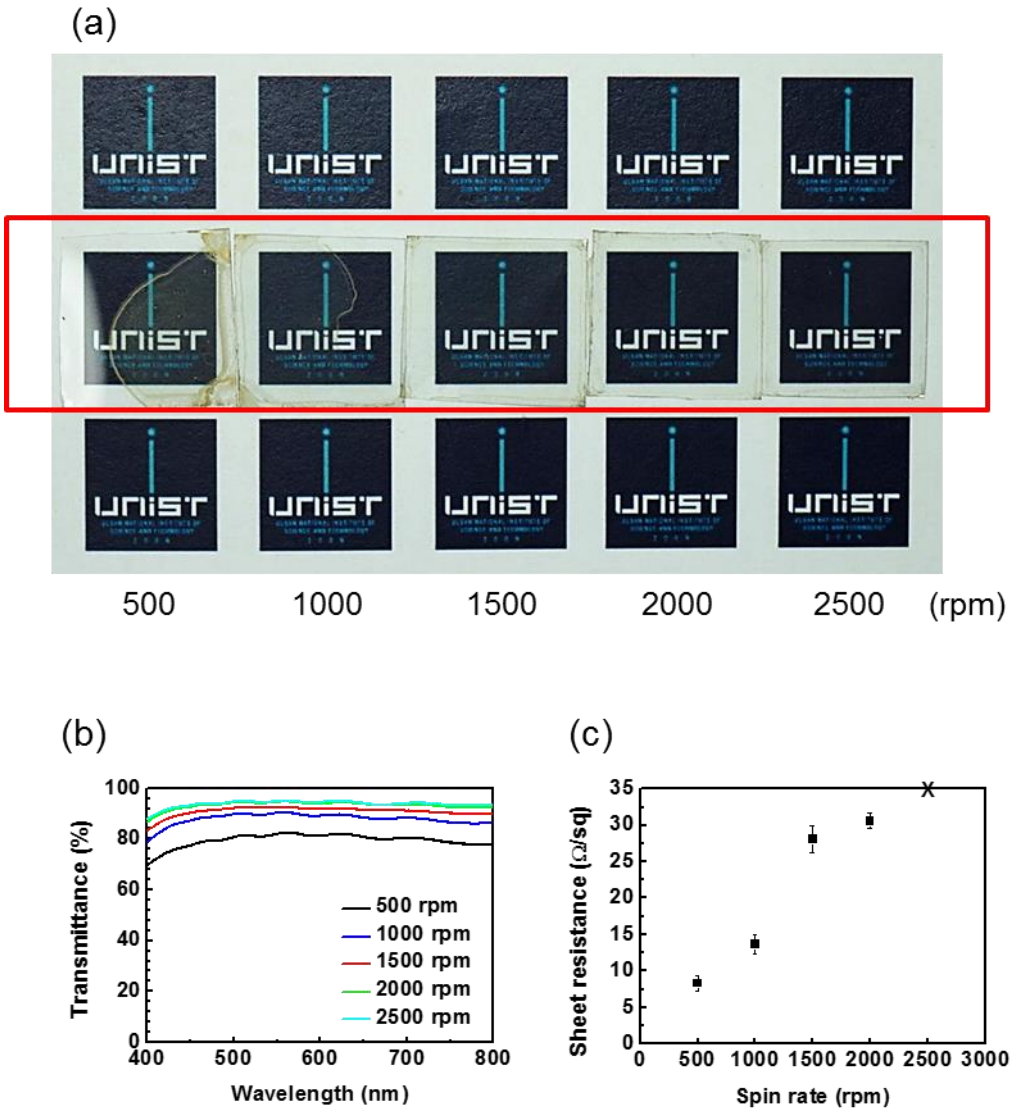

Figure S1. The optoelectronic properties of AgNW percolation networks. (a) The optical images of AgNWs spin-coated on PET film (thickness : 0.1 mm, size of printed mark : 15 mm X 15 mm). AgNWs could not be coated uniformly on a PET film below the spin rate of 1000 rpm. (b) Transmittance of the fabricated AgNWs in terms of spin rates. The coated area was analyzed in case of 500 and 1000 rpm. The spin rate of 1500 and 2000 rpm obtained highly transparent (> 90%) AgNW percolation networks. (c) Sheet resistance of the fabricated AgNWs. Figure 1a corresponds to AgNWs spin-coated with the spin rate of 1500 rpm.

Section S2.

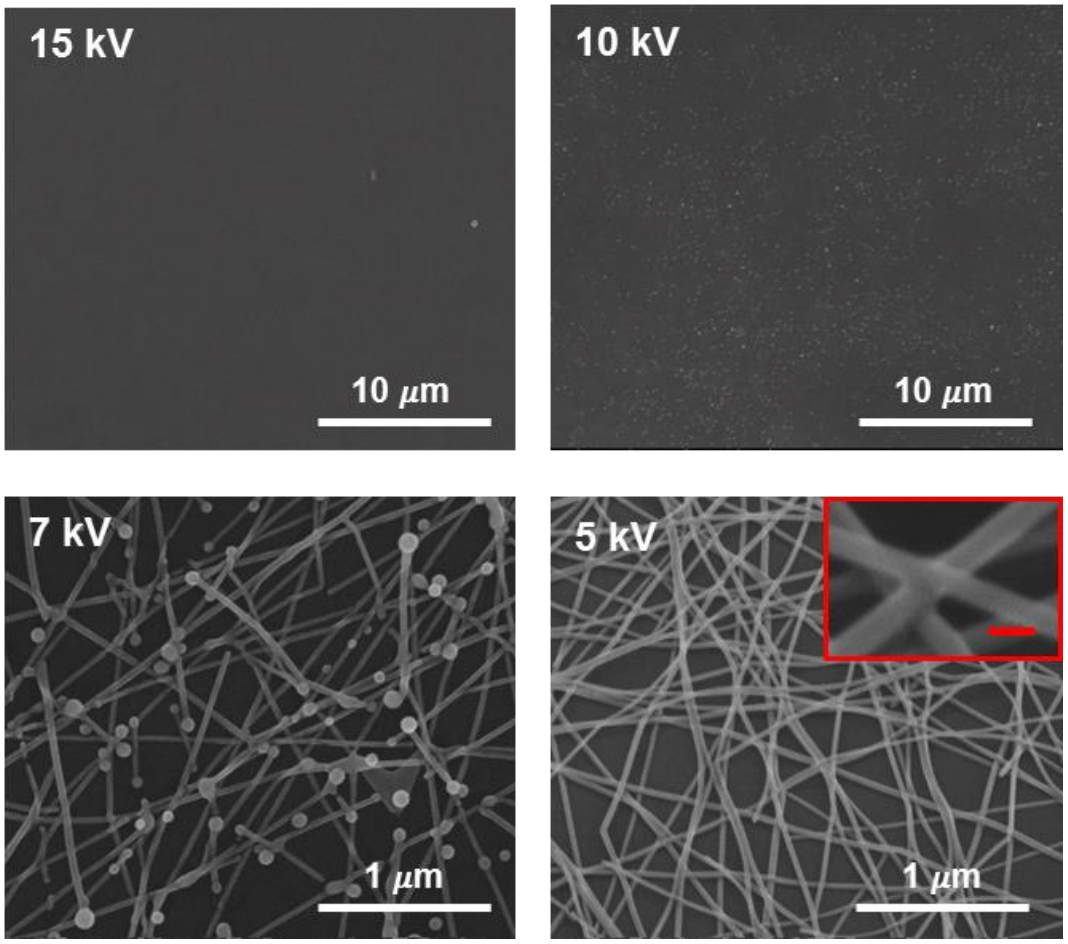

Figure S2. LPEB-irradiated AgNW percolation networks. (Spin rate : 1500 rpm) The red scale bar in inset is 50 nm.

To optimize the acceleration voltage used in LPEB welding, LPEB irradiations with various acceleration voltages were performed on AgNWs. With the 15 kV of acceleration voltage, the spin-coated AgNWs were almost perfectly evaporated. The Ag bubbles were observed following LPEB irradiation with 10 kV acceleration voltage. Using 7 kV, NW-NW junctions were mostly welded; however, Ag bubbles resulted from melting and re-solidification were also emerged at the end of AgNWs. The formation of Ag bubbles with 10 and 7 kV is the same phenomenon to thermal annealing with higher temperature and/or longer time than the optimized condition. Finally, uniformly welded NW-NW junctions were obtained by LPEB irradiation with 5 kV of acceleration voltage. The inset with red border shows the magnified image of welded junction (Figure 2c)

Section S3.

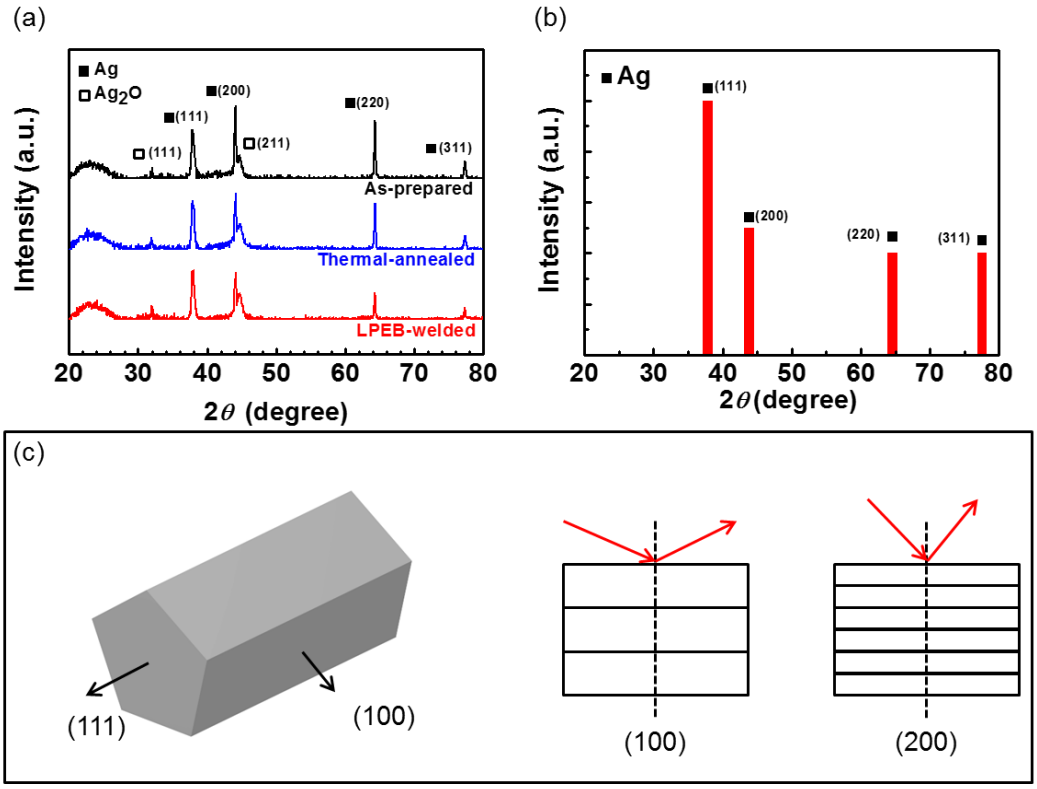

Figure S3. Analysis on crystalline structures of AgNWs. (a) X-ray diffraction peaks from as-prepared, thermal-annealed, and LPEB-welded AgNW percolation networks. (b) The relative intensity of X-ray diffraction peaks from general Ag with nanostructures (JCPDS 04-0783). (c) Schematic diagram of AgNW denoting growing direction.

Generally, Ag with nanostructures should obtain X-ray diffraction peaks have (111) as the main peak as shown in Figure S3b. However, X-ray diffraction peaks on the as-prepared AgNW percolation networks were totally different. This could be contributed from synthesizing NWs into a certain preferred plane, which was verified to be (111) as shown in Figure S3c, to enhance electric conductivity. Although single crystalline structures should show the main peak with overwhelming intensity, the as-prepared AgNW percolation network indicated several peaks as spin-coated AgNWs were dispersed in random directions. The intensity of the (200) peak was the largest in the as-prepared AgNWs indicating AgNWs synthesized into (100) direction. This is simply illustrated in Figure S3c. Following LPEB welding process, relative intensities of X-ray diffraction peaks shifted to the similar shape with Figure S3b, which means that the clear change of crystalline structures after LPEB irradiation was observed.

Section S4.

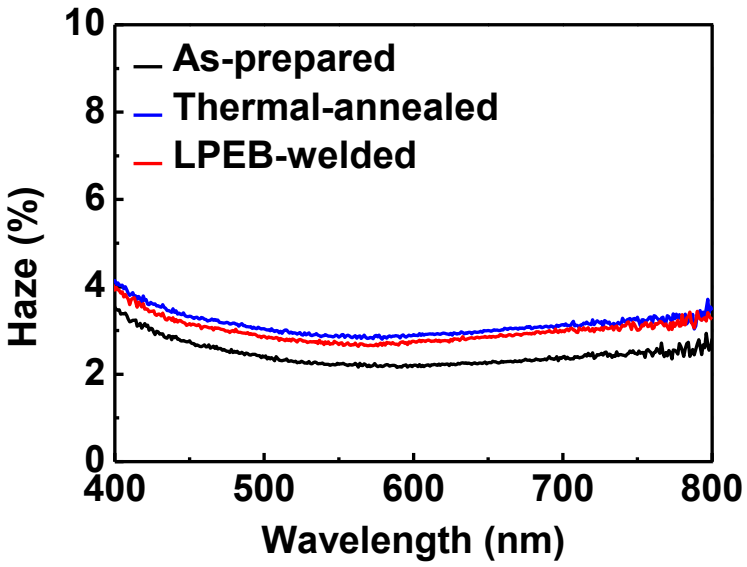

Figure S4. Optical hazeness of as-prepared, thermal-annealed and LPEB-welded AgNW percolation networks.

Section S5.

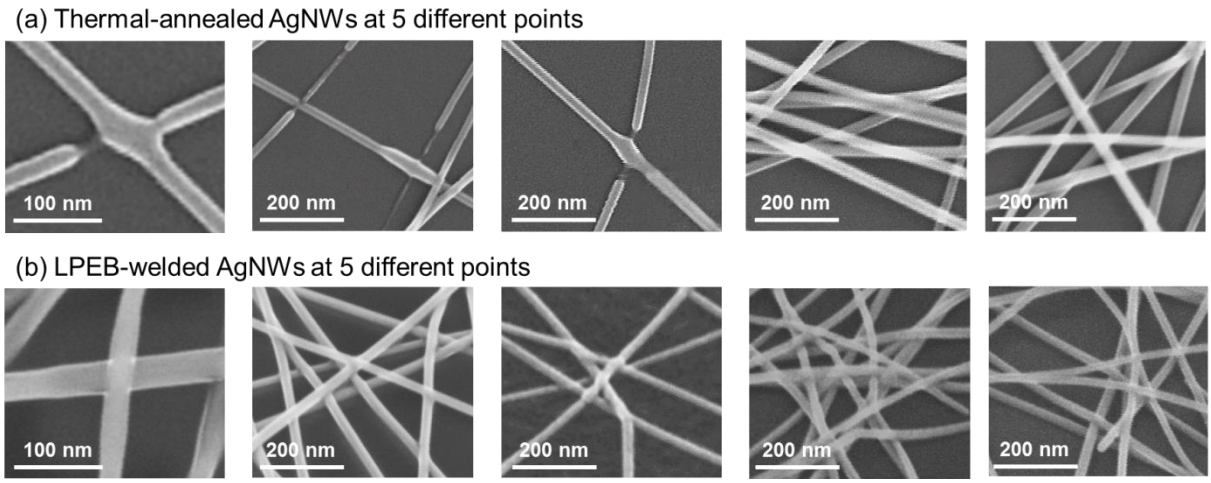

Figure S5. SEM images on AgNWs at five different points in the same sample following (a) thermal annealing and (b) LPEB welding with the optimal condition.

Thermal annealing and LPEB welding have different heat transfer mechanisms. As thermal annealing continuously transfers heat from bottom to top of AgNW percolation networks, whole area of AgNWs receives equal amount of heat though the density of NW-NW junctions are different at each distinct point. Consequently, sparse points of NW-NW junctions could be evaporated due to excessive amount of heat; however, dense junctions were welded or only physically contacted as heat was distributed through the large number of AgNWs (Figure S5a). In case of LPEB irradiation, AgNW itself acts as a heat source. Thus AgNW percolation networks could receive adequate amount of energy to elevate the temperature for welding at both sparse and dense NW-NW junctions with the optimal condition (Figure S5b).

Section S6.

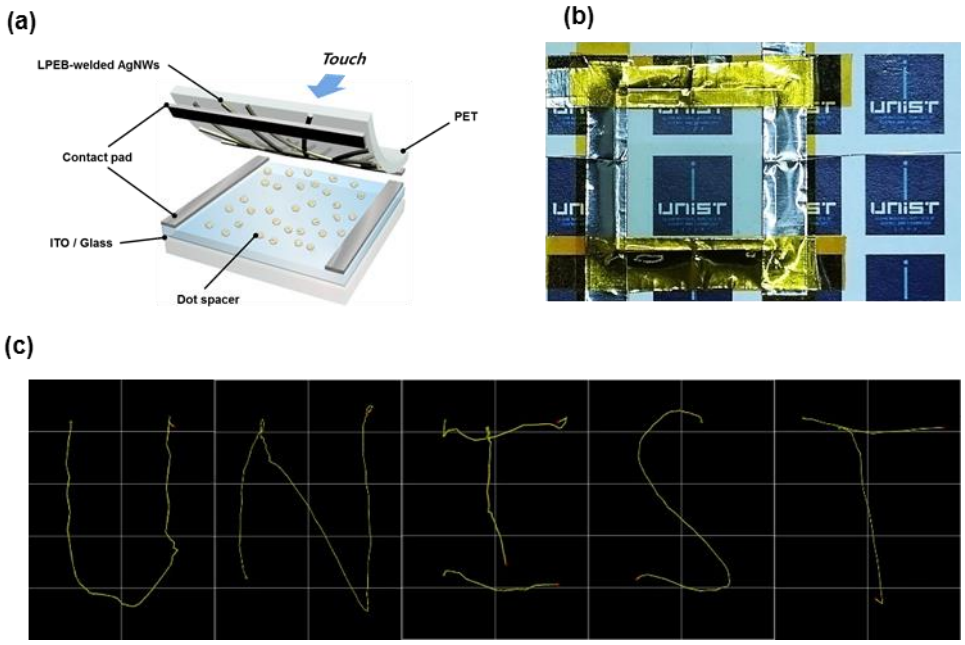

Figure S6. Fabrication of resistive touch-screen panels using LPEB-welded AgNWs. (a) Schematic diagram of the fabricated resistive touch-screen panel. (b) A photograph of the transparent resistive touch-screen panel fabricated using LPEB-welded AgNWs. (c) Demonstration of the touch-screen panel writing the word “UNIST”.

Section S7.

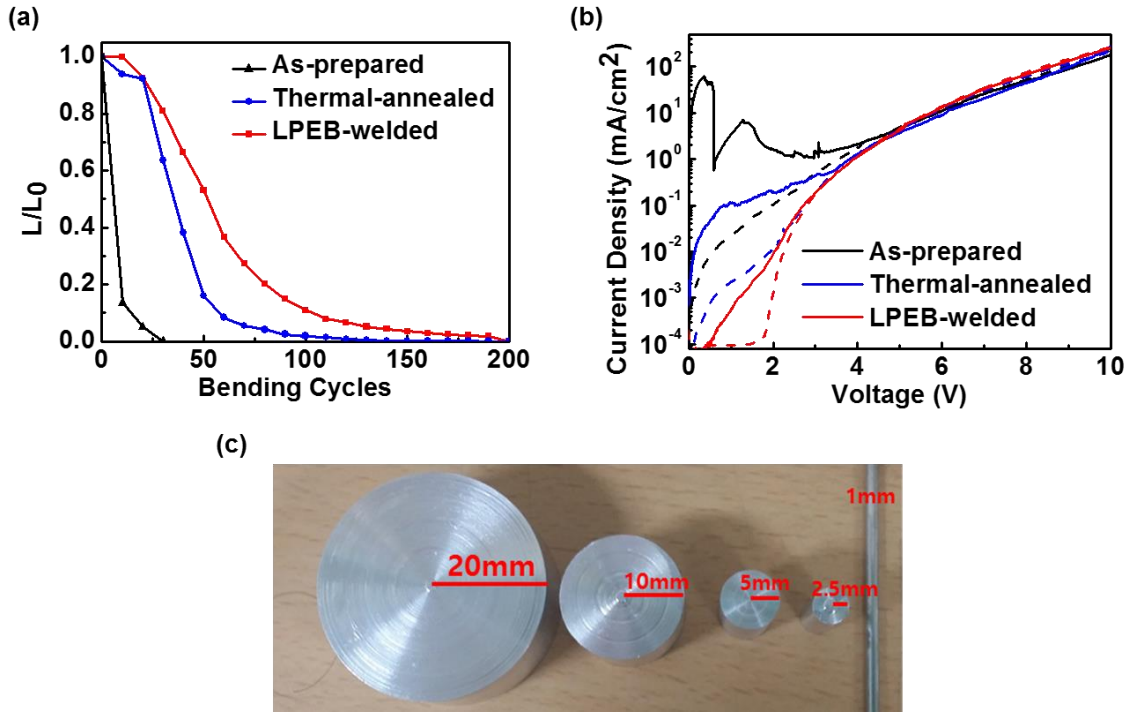

Figure S7. (a) Luminance change of FPLEDs under cyclic bending with 2.5 mm of r_b in ambient conditions. (b) *J-V* characteristics of FPLEDs before and after bending with 0.5 mm of r_b. Dashed lines and full lines in Figure S7(b) denote before and after bending tests respectively. (c) Cylindrical objects for bending test of PLEDs with described r_b.

Section S8.

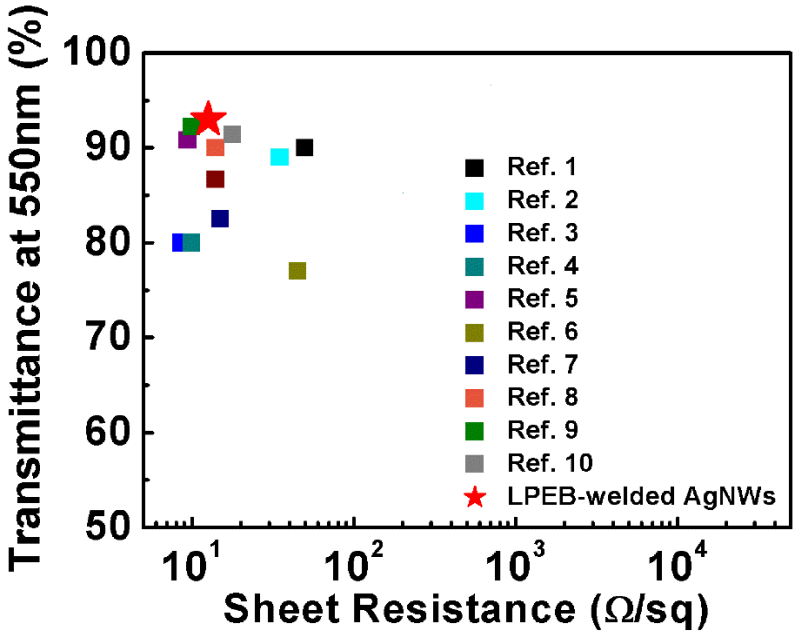

Figure S8. Comparison of our AgNW (red-star) with previously reported transmittance and sheet resistance of AgNWs.

References

1. Scardaci, V.; Coull, R.; Lyons, P. E.; Rickard, D.; Coleman, J. N. Spray Deposition of Highly Transparent, Low Resistance Networks of Silver Nanowires Over Large Areas. *Small* **2011**, 7, 2621-2628.

2. Li, L.; Yu, Z.; Hu, W.; Chang, C. h.; Chen, Q.; Pei, Q. Efficient Flexible Phosphorescent Polymer Light-Emitting Diodes Based on Silver Nanowire-Polymer Composite Electrode *Adv. Mater.* **2011,** 23, 5563-5567.

3. Tokuno, T.; Nogi, M.; Karakawa, M.; Jiu, J.; Nge, T. T.; Aso, Y.; Suganuma, K. Fabrication of Silver Nanowire Transparent Electrodes at Room Temperature. *Nano Res.* **2011,** 4, 1215-1222.

4. Garnett, E. C.; Cai, W.; Cha, J. J.; Mahmood, F.; Connor, S. T.; Christoforo, M. G.; Cui, Y.; McGehee, M. D.; Brongersma, M. L. Self-Limited Plasmonic Welding of Silver Nanowire Junctions. *Nat. Mater.* **2012,** 11, 241-249.

5. Kim, A.; Won, Y.; Woo, K.; Kim, C.-H.; Moon, J. Highly Transparent Low Resistance ZnO/Ag Nanowire/ZnO Composite Electrode for Thin Film Solar Cells. *ACS nano* **2013,** 7, 1081-1091.

6. Preston, C.; Xu, Y.; Han, X.; Munday, J. N.; Hu, L. Optical Haze of Transparent and Conductive Silver Nanowire Films. *Nano Res.* **2013,** 6, 461-468.

7. Liang, J.; Li, L.; Niu, X.; Yu, Z.; Pei, Q. Elastomeric Polymer Light-Emitting Devices and Displays. *Nat. Photonics* **2013,** 7, 817-824.

8. Cheng, T.; Zhang, Y.-Z.; Lai, W.-Y.; Chen, Y.; Zeng, W.-J.; Huang, W. High-Performance Stretchable Transparent Electrodes Based on Silver Nanowires Synthesized via An Eco-Friendly Halogen-Free Method. *J. Mater. Chem. C* **2014,** 2, 10369-10376.

9. Lee, H.; Lee, D.; Ahn, Y.; Lee, E.-W.; Park, L. S.; Lee, Y. Highly Efficient and Low Voltage Silver Nanowire-Based OLEDs Employing A n-Type Hole Injection Layer. *Nanoscale* **2014,** 6, 8565-8570.

10. Nam, S.; Song, M.; Kim, D.-H.; Cho, B.; Lee, H. M.; Kwon, J.-D.; Park, S.-G.;

Nam, K.-S.; Jeong, Y.; Kwon, S.-H. Ultrasmooth, Extremely Deformable and Shape Recoverable Ag Nanowire Embedded Transparent Electrode. *Sci. Rep.* **2014,** 4, 4788 -4794.